








Research Article

Physicochemical, Rheological, Structural, Antioxidant, and Antimicrobial Properties of Polysaccharides Extracted from Tamarind Seeds

Likun Ren ¹, Yang Yang ¹, Xin Bian ¹, Xiaomei Li ¹, Bing Wang ¹,
Dangfeng Wang ^{2,3}, Dan Su ¹, Linlin Liu ¹, Dehui Yu ¹, Xiaoxue Guo ¹,
Xiumin Zhang ^{1,4} and Na Zhang ¹

¹Key Laboratory of Food Science and Engineering of Heilongjiang Province, College of Food Engineering, Harbin University of Commerce, Harbin, Heilongjiang 150028, China

²College of Food Science and Technology, Jiangnan University, Wuxi, Jiangsu 214122, China

³College of Food Science and Technology, Bohai University, National & Local Joint Engineering Research Center of Storage, Processing and Safety Control Technology for Fresh Agricultural and Aquatic Products, Jinzhou, Liaoning 121013, China

⁴Beijing Academy of Food Sciences, Beijing 100068, China

Correspondence should be addressed to Na Zhang; foodzhangna@163.com

Received 20 January 2022; Accepted 1 February 2022; Published 23 February 2022

Academic Editor: Seyed Mohammad Taghi Gharibzahedi

Copyright © 2022 Likun Ren et al. This is an open access article distributed under the Creative Commons Attribution License, which permits unrestricted use, distribution, and reproduction in any medium, provided the original work is properly cited.

In this study, the polysaccharides were firstly extracted from the tamarind seeds in which the crude polysaccharides have been extracted once by hot water extraction. The structure was characterized by FTIR, SEM, and X-ray diffraction after removing protein and small molecule impurities. Furthermore, the rheological and bioactivity of tamarind seed polysaccharides (TSP) were also investigated. The results indicated that the yield of the obtained polysaccharide was 3.42%. TSP was mainly composed of glucose (45.09%), galactose (22.80%), and xylose (28.89%), while it contained characteristic structure of polysaccharides, such as -OH, pyranose, and uronic acid at 3,418, 1,150, and 1,040 cm^{-1} respectively, which demonstrated that it was a uronic acid heteropolysaccharide. Moreover, the XRD pattern revealed the amorphous behavior of TSP, and it was found to consist of films or “sheets” reflected by SEM. The flow behavior testing confirmed its pseudoplastic character, and the flow behavior index (n) was between 0.4539 and 0.9201. The DPPH radical scavenging activity of TSP was 40.34% at 10 mg/mL. Furthermore, TSP displayed moderate hydroxyl radical scavenging and anti-bacterial activities, owing to its special structure and composition. Overall, our results suggested that TSP could be used as a food ingredient with anti-oxidative and antibacterial activities, which provides useful information on the potential utilization of TSP in the food industry.

1. Introduction

The term “gum” is considered to be a group of naturally occurring polysaccharides/carbohydrates derived from a renewable source, which includes plant exudate gum, seed polysaccharide, seaweed polysaccharide, chitosan, and so on [1]. In recent years, polysaccharide gums have received much attention as accessories due to their good functional (water-holding, binding, stabilizing, and emulsifying) properties, and it has been extensively used in many

industries, particularly food field as a gelling agent, emulsifier, and stabilizer [2]. Natural polysaccharide gums are preferred over synthetic ones due to their good features such as biodegradability, nontoxic, sustainability, and availability. In recent years, a lot of polysaccharide gums have been pointed out in the literature from different plant sources and explored for their functional characteristics [3–5].

Tamarind (*Tamarindus indica* L.) belongs to the Leguminosae family and is widely distributed in South Asian and Southeast Asian countries such as India and Thailand [6].

The flower and leaf are consumed as vegetables, while the pulp is used as a raw material to produce snack foods, such as tamarind cake, beverages, and so on [7]. With the increasing popularity of Tamarind products, a great expansion of production leads to a large number of by-products (tamarind seeds) being produced, resulting in environmental pollution and waste of resources. Therefore, the recycling of tamarind seeds is helpful to improve sustainability in the food industry and reduce environmental pollution [8]. Currently, some researchers have processed tamarind seed to extract polysaccharides and characterized their functional and structural properties [9–11]. For structures, Shao et al. [11] pointed out that TSP obtained by water extraction and alcohol precipitation is a mixed polysaccharide composed of glucose, xylose, and galactose, which contains uronic acid. Moreover, TSP possesses a wide range of biological activities such as anti-inflammation, antiobesity, and immune protection [12, 13]. Besides, some researchers have confirmed that natural seed polysaccharides can be used as a potential anti-microbial agent to be applied in the food industry [14–16]. The presence of uronic acid in TSP makes it possible to be a potential anti-bacterial agent. However, the anti-bacterial activity of TSP has not been reported.

Tamarind seeds will be discarded when polysaccharides or other substances were obtained. In our previous study, the waste tamarind seed after extracting polysaccharides still showed high polysaccharide content, indicating that this industrial waste still contains polysaccharides. However, until now, little information is available on the utilization of these wastes. The exploration of extraction and functional properties of these polysaccharides is one of the most important challenges in the food industry, which can further realize the efficient utilization of tamarind seed resources. Based on this, the present study is to further obtain and purify the TSP from these tamarind seeds that have been extracted polysaccharides once, characterizing structures by composition analysis, SEM, FT-IR, XRD, and rheological assay. Furthermore, the bioactive (antioxidant activity and antimicrobial) properties of TSP were evaluated. These results were compared with the tamarind polysaccharide that has been reported to help fully utilize the tamarind seed and guide the potential application of TSP as a pharmaceutical supplement or functional food ingredient.

2. Materials and Methods

2.1. Materials and Chemicals. Tamarind seed powder was provided by Yunnan Maoduoli Group Food Co. Ltd. (Yuxi, China). The monosaccharide standards were all of chromatography grade with purity >99%. All monosaccharide standards, trifluoroacetic acid, acetic acid sodium salt, and chromatography-grade methanol were obtained from Sigma Chemical Co. (St. Louis, MO, USA). Other chemicals used in the study (e.g., Congo Red reagent, phenol, chloroform, ferrous sulfate, DPPH, salicylic acid, etc.) were of analytical grade. All solutions were prepared using distilled water, and ultrapure water was obtained from a Milli-Q water purification system.

Brain heart infusion broth (BHI) was purchased from Yinuo Biotechnology Co. Ltd., and agar was used, which

were obtained from Shanghai Merck Chemical Technology Co. Ltd. (Shanghai, China).

2.2. Preparation of TSP. The tamarind seed polysaccharides (TSP) were extracted by water and precipitated by ethanol according to the methods described by Chai and Zhao [17] with modifications. The tamarind seed powder (5.00 g) was dissolved in the distilled water at a mass ratio of 1:50 and then kept at 90°C for 50 min with constant stirring. The solution was further allowed to stand for 24 h and centrifuged at 4,000 rpm for 20 min. The supernatants were mixed with the same volume of 95% ethanol, stirring and standing for 24 h; the precipitate was obtained after washing with 95% ethanol 5 times and dried at 40~45°C as crude polysaccharides.

2.3. Purification of TSP. The free protein in the crude polysaccharides was removed by employing the method of Seavage [18]. The crude polysaccharides (2.00 g) were dissolved in distilled water (200 mL) and mixed with four volumes of Seavage reagent (chloroform/n-butanol, V/V = 4:1) at 25°C. Following centrifugation (TDL5M, Kaldasy Co. Ltd, Changsha, China) at 7,000 rpm for 15 min at room temperature, the up-layer solution was collected, and the above procedure was repeated until the protein layer disappears completely. All polysaccharides were collected and precipitated with ethanol. Subsequently, the precipitate was redissolved in water and was dialyzed (MW 3500 Da) against flow tap water for 48 h and distilled water for 12 h. The TSP was obtained by lyophilization treatment. The polysaccharide yield (% w/w) was calculated as follows:

$$\text{polysaccharide yield (\%)} = \frac{W_1}{W_0} \times 100, \quad (1)$$

where W_1 and W_2 were the weight of the freeze-dried sample and the raw material, respectively.

Protein content was performed as described by Jahanbin et al. [19] using a Kjeldahl apparatus. The protein removal rate was calculated as follows:

$$\text{protein removal rate (\%)} = \frac{A_1 - A_2}{A_1} \times 100, \quad (2)$$

where A_1 and A_2 were the protein content of crude TSP and purified TSP, respectively.

The TSP was added to distilled water to a final concentration of 1 mg/mL. The full ultraviolet scan of TSP was obtained in the wavelength range of 190–400 nm.

2.4. Chemical and Monosaccharide Composition Analysis. The total carbohydrate content of TSP was measured by the phenol sulfuric acid method, and glucose was used as standard [20]. Uronic acid content was determined via meta-hydroxydiphenyl analysis [21].

The monosaccharide composition of TSP was determined using a Thermo ICS5000+ system (Thermo Fisher Scientific, Waltham, MA, USA) with fucose (Fuc), rhamnose (Rha), arabinose (Ara), galactose (Gal), glucose (Glu), xylose

(Xyl), mannose (Man), fructose (Fru), ribose (Rib), galacturonic acid (Gal-UA), glucuronic acid (Glc-UA), manuronic acid (Man-UA), and guluronic acid (Gul-UA) as the standards. Briefly, 5.00 mg TSP was dissolved in trifluoroacetic acid (TFA) solution at 121°C for 2 h and blow-dried with nitrogen. Then mixed with methanol clean and blow-dried for 3 times. The TSP was redissolved with ultrapure water and filtered through a 0.22 μm membrane filter for instrument detection. A Dionex™ CarboPac™ PA10 (4.0 mm \times 250 mm, 10 μm , Thermo Fisher Scientific, USA) was used to identify the composition and kept at 30°C during operation. The 10 μL sample was injected; then using A-H₂O and B-NaOH (100 mM) as mobile phase, monosaccharide compounds were eluted under the conditions, which were shown in Table 1.

2.5. Triple-Helical Structure Determination of TSP. The conformation structure of TSP was determined using the Congo red method reported by Wang et al. [22]. The TSP solution (1 mg/mL) containing 80 μM Congo red solution was mixed in NaOH solution with final concentrations ranging from 0 M to 0.5 M. A UV spectrometer (T6, Beijing Puxi General Instrument Co. Ltd., Beijing, China) was used to scan the absorbance ranging from 190 nm to 600 nm after being kept for 30 min at room temperature and record the maximum absorption wavelength.

2.6. Particle Size and Zeta Potential Measurements of TSP. The particle size and zeta potential measurements were measured by dynamic light scattering (DLS; Zetasizer nano-ZSE 900, Malvern Instruments Co. Ltd., United Kingdom). The TSP powder was diluted in ultrapure water to the desired concentration (2.00 mg/L). The measurement was performed in triplicate at a room temperature of 25°C [23].

2.7. Morphologic Observation of TSP. The morphologic characterization of TSP was observed by scanning electron microscope (SEM; SU8010, Hitachi Ltd., Japan) after coating with gold by a plating instrument. The accelerated voltage was 10.0 kV with enlargement multiple 100, 500, 2,000, and 10,000.

2.8. Fourier Transform Infrared (FT-IR) Spectroscopic Assay of TSP. The sample was mixed with KBr with a ratio of 1:50 and then pressed into 1 mm pallets. The infrared spectrum of TSP was recorded using a Thermo Fisher Scientific Nicolet 6700 FT-IR Spectrometer (Thermo Fisher Science, USA) during the range of 4,000–400 cm^{-1} at room temperature.

2.9. X-Ray Diffraction of TSP. An X-ray powder diffractometer (Bruker D8 Advance, Germany) was used to determine the degree of TSP crystallinity with Cu K α radiation ($\lambda = 1.78901 \text{ \AA}$) with a source running at 40 kV and 40 mA, respectively. The figure was obtained in the diffraction angle 5–90° (2 θ), with a speed of 3°/min and a step of 0.02°.

TABLE 1: The eluted conditions of the monosaccharide composition.

Time (min)	Flow rate (min)	A mobile phase (%)	B mobile phase (%)
0.0	0.5	97.5	2.5
30.0	0.5	80	20
30.1	0.5	60	40
45	0.5	60	40
45.1	0.5	97.5	2.5
60	0.5	97.5	2.5

2.10. Rheological Properties of TSP. All rheological properties of TSP were performed by TA-AR 2000 controlled-stress rheometer (TA Instruments Inc., New Castle, DE, USA) equipped with a 40 mm diameter stainless steel parallel plate. The flow curves of the various concentrations of TSP solution (1, 3, 5, 10, 15, and 20 mg/mL) were determined with shear rate ranging from 0.01 s^{-1} to 1,000 s^{-1} at 25°C. The consistency coefficient (K) and the flow behavior index (n) were calculated by the power-law model as follows:

$$\tau = K(\dot{\gamma})^n, \quad (3)$$

where τ is shear stress (Pa), K is the consistency index ($\text{Pa}\cdot\text{s}^n$), $\dot{\gamma}$ is the shear rate, and n is the flow behavior index.

2.11. In Vitro Antioxidant Activity of TSP

2.11.1. DPPH Radical Scavenging Activity Assay. DPPH (2,2-diphenyl-1-picrylhydrazyl) free radical scavenging activity was measured as reported by Zhang et al. [24] with several modifications. The TSP solutions (2.0 mL) of different concentrations were added to 2.0 mL of a methanolic solution of DPPH radical (0.2 mmol/L). The absorbance of the mixture was measured at 517 nm after incubated for 30 min in dark at room temperature. The common anti-oxidants-ascorbic acid and the reaction solution without TSP were used as the positive and negative control, respectively. Radical scavenging activity was calculated as follows:

$$\text{DPPH scavenging activity (\%)} = \frac{A_0 - A_1}{A_0} \times 100, \quad (4)$$

where A_0 is the absorbance of reaction solution without TSP and A_1 is the absorbance of the test sample.

2.11.2. Hydroxyl Radical Scavenging Activity. A 2.0 mL TSP solution (1, 2, 5, 10, 15, and 20 mg/mL) was mixed with 1.0 mL of 1.5 mmol/L FeSO₄, 0.7 mL of 6 mmol/L H₂O₂, and 0.3 mL of salicylic acid. The mixture was heated in the water bath at 37°C for 1 h, and then the absorbance at 510 nm was measured. The scavenging rate was calculated by the following equation:

$$\text{scavenging rate (\%)} = \left[1 - \frac{A_1}{A_0} \right] \times 100, \quad (5)$$

where A_0 is the absorbance of control and A_1 is the absorbance of the sample.

2.12. Antibacterial Activity of TSP. The anti-bacterial activity of TSP was assessed by the Oxford cup method described by Wang et al. [18] with some modifications. Briefly, 10 mL of an overnight culture of *Escherichia coli* were mixed 200 mL brain heart infusion broth (BHI) nutrient agar in well plates. After solidification, the Oxford cup was pulled out, and 200 μ L TSP solution (20 mg/mL) was injected into the hole for the Oxford cup. The control and positive groups were treated with sterile dH₂O and chitosan (20 mg/mL). The Petri dishes were incubated at $37 \pm 1^\circ\text{C}$ for 24 h, and the inhibition zones were observed.

2.13. Statistical Analysis. All experiments were done in triplicate to get mean values \pm standard deviations. Statistical analysis was conducted using a one-way analysis of variant (ANOVA) by the SPSS 20.0 (SPSS Inc., Chicago, IL, USA). A probability value of $p < 0.05$ was considered to be statistically significant.

3. Results and Discussion

3.1. Extraction and Purification of Polysaccharides. After standing in 95% ethanol solution for 24 h, the morphology of TSP subjected to ethanol precipitation is shown in Figure 1(a). The TSP was loose and porous and floats on the ethanol. The Sevage solution can denature protein and promote the separation of protein and polysaccharides. There were three layers after centrifuging of the mixed solution (TSP and Sevage solution), namely, TSP on the top, followed by protein and Sevage solution (Figures 1(b) A). After repeated Sevage operation 5 times, the protein layer disappeared (Figure 1(b): B). Furthermore, the UV detector was used to observe the removal of protein, and the results were displayed in Figure 1(c). The crude TSP with absorption peaks was observed at 280 nm, while the TSP treated with the Sevage solution lacks absorption in the range of 275–300 nm. The results suggested that protein has been removed, and the protein content analysis indicated that the removal rate of protein was 86.67%. Tamarind polysaccharide was obtained by purification and freeze-drying (Figure 1(d)). The yield of the obtained polysaccharide was 3.42%.

3.2. Chemical and Monosaccharide Composition Analysis of TSP. The TSP was low in protein (1.31%) and uronic acid (1.26%). The total carbohydrate content of TSP was 89.13% (Table 2), indicating that the purity was relatively high in this study. The composition of TSP was consistent with a previous report of Li et al. [25]. The content of uronic acid was different from the existing reports (5.4% uronic acid), which may be related to the conditions for the first extraction of polysaccharides.

The results of monosaccharide compositions of TSP were determined by HPAEC, and the results were displayed in Figure 2. According to the retention time of monosaccharides standard mixture in chromatography system, the retention times of 13 kinds of standard monosaccharide samples (Fuc, Rha, Ara, Gal, Glc, Xyl, Man, Fru, Rib, Gal-UA, Gul-UA, Glc-

UA, and Man-UA) were 2.841, 7.200, 7.608, 9.575, 10.983, 12.916, 13.950, 15.608, 17.175, 33.908, 34.650, 36.441, and 38.683, respectively. Moreover, compared with the standard mixture, the TSP contained 7 kinds of monosaccharides, and the content of glucose was the highest in TSP, followed by Xyl, Gal, Ara, Fru, Glc-UA, and Gal-UA (Figure 2) and no Fuc, Rha, Man, Rib, Gul-UA, and Man-UA were observed in TSP. There were some differences with the finding of Gidley et al. [26] on the molar ratio of Glu:Gal:Xyl (1.97:1.00:1.31). This might be related to the raw material and preparation method of TSP. In this study, the tamarind seed powder that has been used for the extraction of polysaccharides was used as raw material to further extract the remaining polysaccharide to realize the full utilization of industrial waste. Furthermore, the monosaccharide composition and content of TSP play an important role in its functional and biological properties. Glucose can supplement the energy of the body. On the contrary, xylose cannot be absorbed and is considered to be the best suitable monosaccharide for obese individuals. Besides, xylose can activate intestinal *Bifidobacterium* and promote its growth [27]. Due to the presence of glucose and xylose, TSP can be used in the food industry as a high-quality polysaccharide, which can endow food with sweetness and biological activity.

3.3. Triple-Helical Structure of TSP. Congo red dye can form complexes with polysaccharides content triple-helical structure to influence the visible absorbance maximum, which were used to detect the triple-helical structure of polysaccharides [28]. It can exhibit a bathochromic shift when a tertiary structure of polysaccharides was formed. In contrast, the trend of maximum absorbance wavelength was similar with Congo red solution to a shorter wavelength when the tertiary-helical structure does not exist. [22]. Figure 3 shows the change of the max absorbance of the TSP under NaOH solution with concentrations were 0–0.5 M. In Congo red tests (Figure 3), there were significant shifts in the maximum absorption wavelength of TSP and the values from 499 nm to 486 nm with the increasing NaOH concentration. Moreover, the changing trend was almost similar to that of the Congo red. This observation was in accordance with a previous report by Mao et al. [29], who found that crude polysaccharides are not easy to form triple helix structure. Therefore, it could be concluded that triple-helical does not exist in TSP.

3.4. Particle Size and Zeta Potential of TSP. The ζ potential and particle size are good indicators of the colloid system stability. In general, the particles can disperse or dissolve in the system when the particles have a small size and large negative or positive zeta potential [30]. The ζ potential and particle size of TSP were 922.7 ± 32.51 nm and -4.87 ± 0.20 mV, respectively. The findings of particle size were consistent with the finding of Crispin-Isidro et al. [28]. The polydispersity index (PDI) is used to indicate the uniformity of particle size distribution, the value < 0.3 was considered a uniform distribution; the value > 0.3 was characteristic of system uneven distribution, and the degree

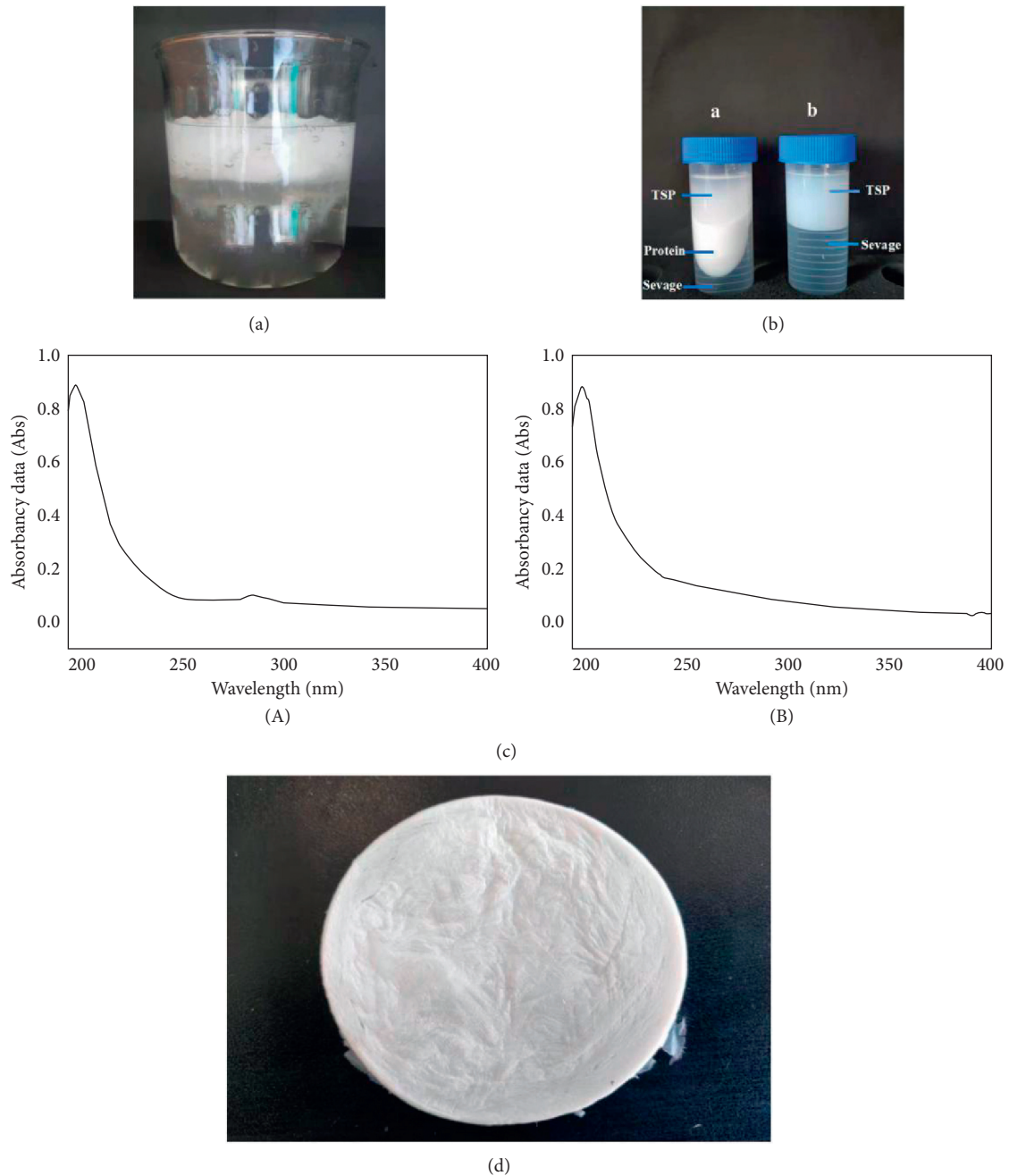


FIGURE 1: Preparation, purification, and acquisition of TSP. (a) The solution was precipitated with 95% (v/v) ethanol at 4°C overnight. (b) Deproteinization: (A) remove protein of TSP by Sevage solution for the first time and (B) remove protein of TSP by Sevage solution for the fifth time. (c) Scan of TSP during the range of 190–400 nm: (A) crude polysaccharides and (B) TSP after removing impurities. (d) TSP (impurities removal) lyophilized sample.

of nonuniformity increases with the increase of PDI value [31]. The PDI (0.32) in this study indicated that the TSP solution was uneven. Moreover, the TSP solution was negatively charged, suggesting that TSP contains uronic acid, but the ζ potential value of TSP (-4.87 mV) was significantly smaller than the previously reported value from Crispín-Isidro et al. [28]. This may be due to the purification step. The purification operations can remove more charged compounds, for instance, the protein impurities removed during purification improved the ζ potential value [23].

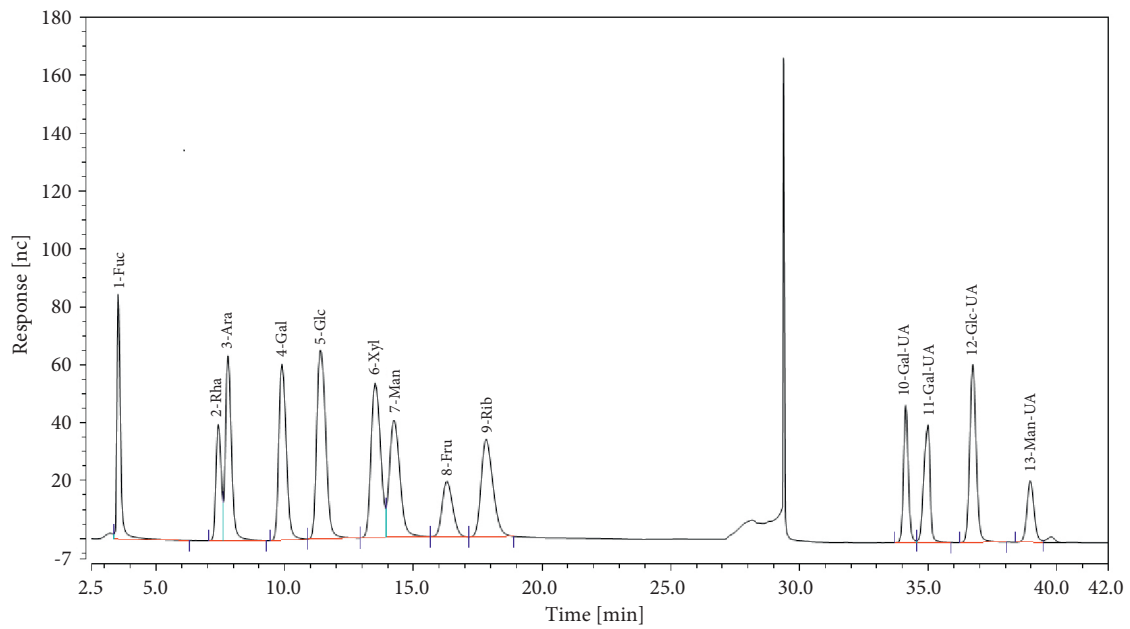
Overall, our results suggested that TSP were potential compounds that contain uronic acid and exhibit good stability of the solution.

3.5. Morphologic Observation. The SEM photograph of TSP was shown in Figure 4. As presented in Figures 4(a) and 4(b), the morphology of TSP was smooth and sheet. The shape of the TSP mainly exhibited leaf structure with some holes. As seen from the image at 2,000-fold magnification

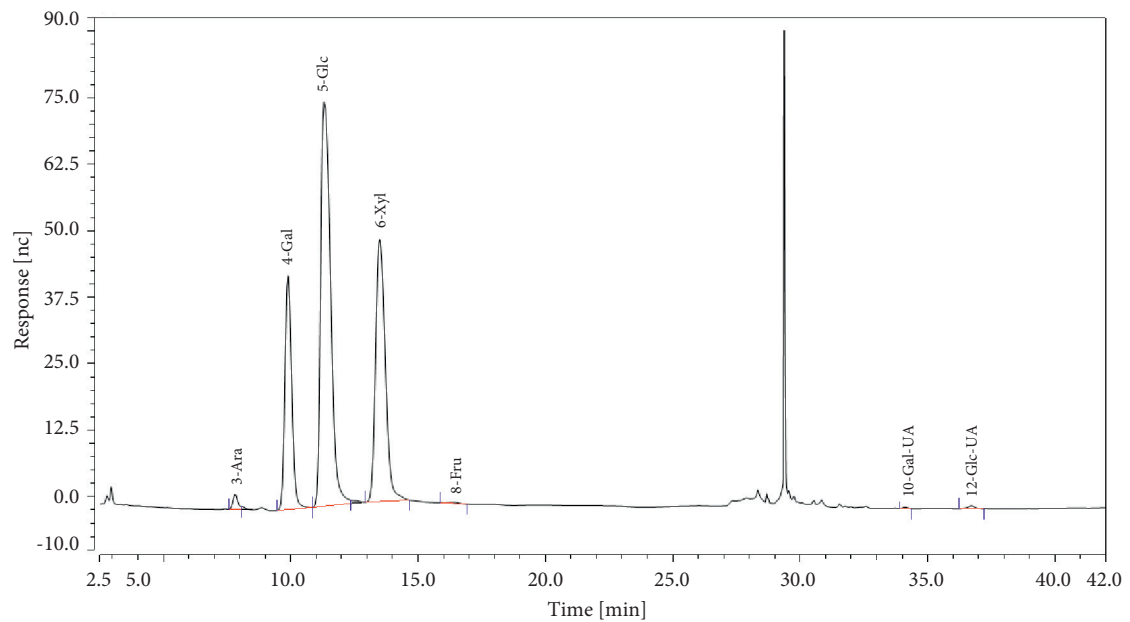
TABLE 2: Chemical and monosaccharide composition of polysaccharides extracted from TSP.

Compound	Content (%)
Protein	1.31 ± 0.2 ^d
Total carbohydrate	89.13 ± 0.27 ^a
Uronic acid	1.26 ± 0.03 ^d
Glucose (Glc)	45.09 ± 1.21 ^b
Xylose (Xyl)	28.89 ± 0.43 ^c
Galactose (Gal)	22.80 ± 0.52 ^c
Arabinose (Ara)	1.28 ± 0.03 ^d
Fructose (Fru)	0.44 ± 0.01 ^e
Glucuronic acid (Glc-UA)	0.33 ± 0.00 ^e
Galacturonic acid (Gal-UA)	0.17 ± 0.00 ^f

a–f: statistical significance level of $p < 0.05$ calculated by Duncan's test.



(a)



(b)

FIGURE 2: High-performance anion-exchange chromatography (HPAEC) of TSP: (a) HPAEC chromatography of standard mixture with glucose, xylose, galactose, arabinose, fructose, glucuronic acid, glucuronic acid, fucose, rhamnose, mannose, ribose, mannanuronic acid, and guluronic acid and (b) HPAEC chromatography of TSP.

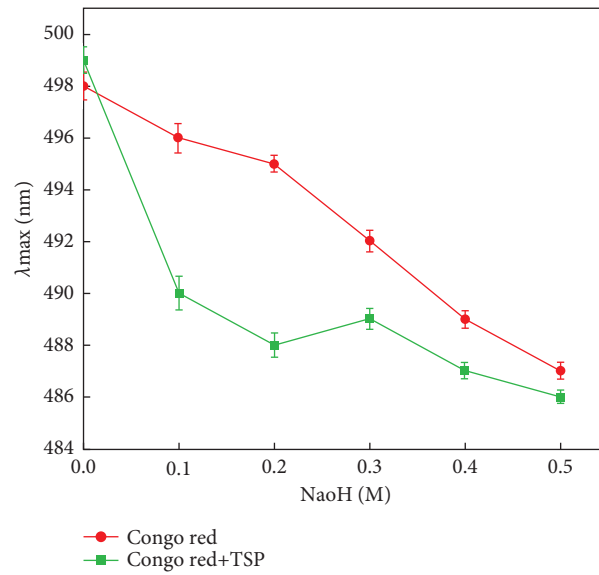


FIGURE 3: Plots of the maximum absorption of Congo Red and TSP Congo Red complex at various concentrations of NaOH. Statistical significance level of $p < 0.05$ calculated by Duncan's test.

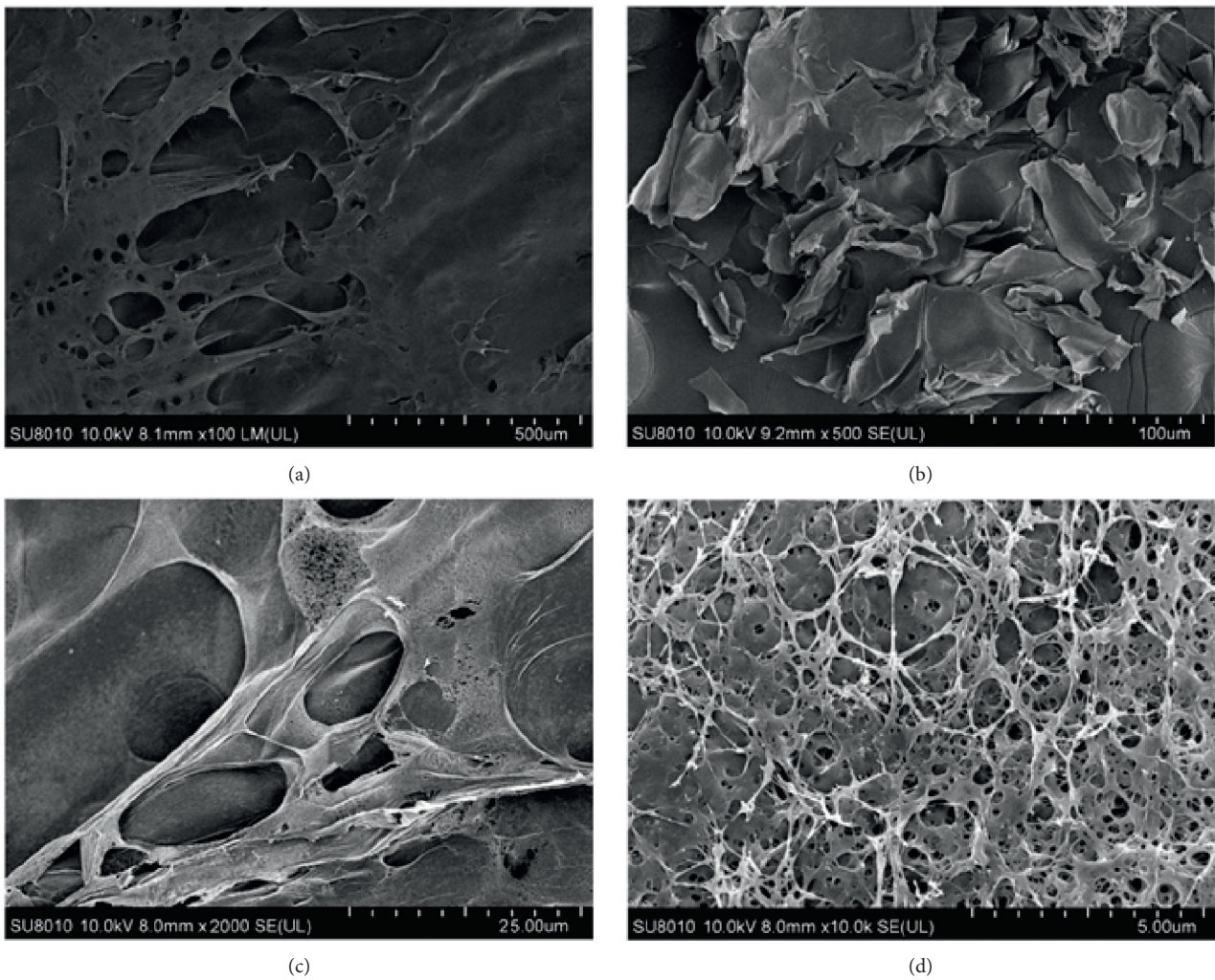


FIGURE 4: Scanning electron microscope image of TSP obtained from magnification 100x (a), 500x (b), 2,000x (c), and 10,000x (d).

(Figure 4(c)), there were many holes on the surfaces of TSP sheets. Furthermore, the photograph at 10,000-fold magnification suggested that TSP showed a rough, tight, and uneven reticular surface (Figure 4(d)). The SEM images suggested that the method of preparation and purification in this paper lead to the surface of TSP forming several irregular “sheets” shapes. However, mesh structures were formed inside by the cross-linking of polysaccharides molecules. Furthermore, the pores present in the sample may be related to the lyophilization process [32].

3.6. Fourier Transform Infrared. The FT-IR was performed to further characterize the tamarind seed polysaccharides. As shown in Figure 5(a), the picture displays all typical peaks and bands associated with polysaccharides. The wide absorption peak at about $3,418\text{ cm}^{-1}$ corresponded to the stretching vibration of hydroxyl groups (O–H) induced by inter- or intramolecular, which was considered to be characteristic of polysaccharides [33, 34]. The peak observed at $2,970\text{ cm}^{-1}$ and $2,900\text{ cm}^{-1}$ were probably due to the C–H stretching and bending vibrations including CH, CH_2 , and CH_3 [35]. Furthermore, some peaks from $1,400\text{ cm}^{-1}$ to $1,200\text{ cm}^{-1}$ are also related to C–H bands; for instance, the peak at $1,370\text{ cm}^{-1}$ and $1,246\text{ cm}^{-1}$ in this paper was exhibited by CH_2 bending vibrations. Besides, Tang et al. [36] pointed out that the signal at $1,246\text{ cm}^{-1}$ might be related to the asymmetrical stretching vibration of S=O, evidence of the sulfated group. However, the C–OO symmetric stretching vibration takes place within the wavelength at $1,623\text{ cm}^{-1}$. The change in C–OO could affect the functional properties by providing ions binding sites. The presence of pyranose was determined in $1,150\text{ cm}^{-1}$ and $1,078\text{ cm}^{-1}$, a characteristic band of carbohydrates, where $1,078\text{ cm}^{-1}$ was ascribed to the C–O stretching vibration in the pyranose ring structure of C–O–H [37]. The sharp and strong absorption peak at $1,040\text{ cm}^{-1}$ was assigned to the pyranose-form sugars and could be related to the presence of uronic acid. This result supported the test of TSP composition. Some studies have confirmed that polysaccharides containing uronic acid possess good rheological properties. TSP with uronic acid might also have rheological properties. Moreover, the $1,040\text{ cm}^{-1}$ wave number could be associated with C–N as well as indicated the presence of protein in TSP. It is evident that the purification did not completely remove the protein present in TSP, and there were some proteins in TSP. These results were consistent with the 86.67% deproteinization rate determined and 1.31% protein content in this experiment. According to the report of Yang and Zhang [38], the absorption in the region of 920 cm^{-1} resulted from α -glycosidic bond, and the peaks at 683 cm^{-1} and 579 cm^{-1} correspond to the β -glycosidic bond. These findings showed that TSP is a heteropolysaccharide containing uronic acid, sulfated group, and α - and β -glycosidic bond.

3.7. Crystallinity. The XRD was used to investigate the crystallography of polysaccharides; the results were shown in Figure 5(b). There was a broad peak spanning 2θ from 10° to 35° , and a peak being observed at approximately 19.62° , 2θ revealed that TSP had a typical XRD pattern for non- or semicrystalline polymers [18], and it is an

amorphous material. Studies with other polysaccharides detected crystallinity very similar to the result in this paper, which was very common in polysaccharides of nature [39]. Basu et al. [40] studied the polysaccharide from *Dolichos biflorus* Linn. and *Trachyspermum ammi* Linn. seeds structure, and the same presented crystallinity similar to the amorphous as observed for TSP in this present study.

3.8. Rheological Behavior Analysis Relation. Figures 6(a) and 6(b) presented the relationship between apparent viscosity/shear stress and shear rate for different concentrations of TSP solutions at 25°C . As shown in Figure 6, the viscosity of TSP at various concentrations decreased gradually with increasing shear rate that showed typical pseudoplasticity of shear thinning of the TSP, since the chains of polysaccharide molecules become aligned in the flow direction, generating solutions with lower viscosity, resulting in less interaction among adjacent polymer chains [41]. But the change rate of viscosity was different with different TSP concentrations. High diminution was obtained, when the sample concentration was increased. Moreover, in the shear rate from 0.01^{-1} to $1,000^{-1}$, the increased TSP concentration led to an increase in viscosity. This result was likely due to an increase of molecular number per unit volume, resulting in increased entanglement and aggregation of macromolecule chains at higher concentrations, which would exhibit higher viscosity [42]. With the increase of shear rate, the stress curve (Figure 6(b)) shows the opposite trend to the viscosity curve. At all the concentrations, the stress of the TSP solution increased with the increase of shear rate, which also indicated the shear-thinning behavior of the solution.

The curve was fitted to a power-law equation, and the relevant ones are listed in Table 3. The value of the flow behavior index (n) was a symbol to explain the liquidity property of the sample. For $n < 1$ it was a pseudoplastic fluid. The value of $n = 1$ behaved as a Newtonian fluid, and it stands for a dilatant fluid when $n > 1$. The shear-thinning behavior of the TSP solution could be explained by the power-law equation. It was noticed from Table 3 that “ n ” of the TSP solutions was between 0.4539 and 0.9201 and the “ n ” value of TSP solutions tended to be equal to one when the concentration was higher, which indicated that the TSP solution fluid gradually turns into Newtonian fluid, exhibiting a slimy appearance. The variation of “ n ” value with concentration was related to a reversible “structure” that formed under “rest” or equilibrium conditions [43]. Furthermore, the molecules in high concentration TSP solution began to overlap and form an intermolecular connection or “connection region,” which restricted the movement and stretching of the polymer chain in the aqueous system. Therefore, the viscosity increased significantly with the increase of mass concentration. This observation was consistent with the report by Alpizar-Reyes et al. [44], who found tamarind seed gum exhibited a similar tendency.

As shown in Figure 6(c), different concentrations of TSP solution were placed in the test tube to observe the sample state. With the increase of concentration, the transparency of the TSP solution decreased, and the viscosity of the TSP

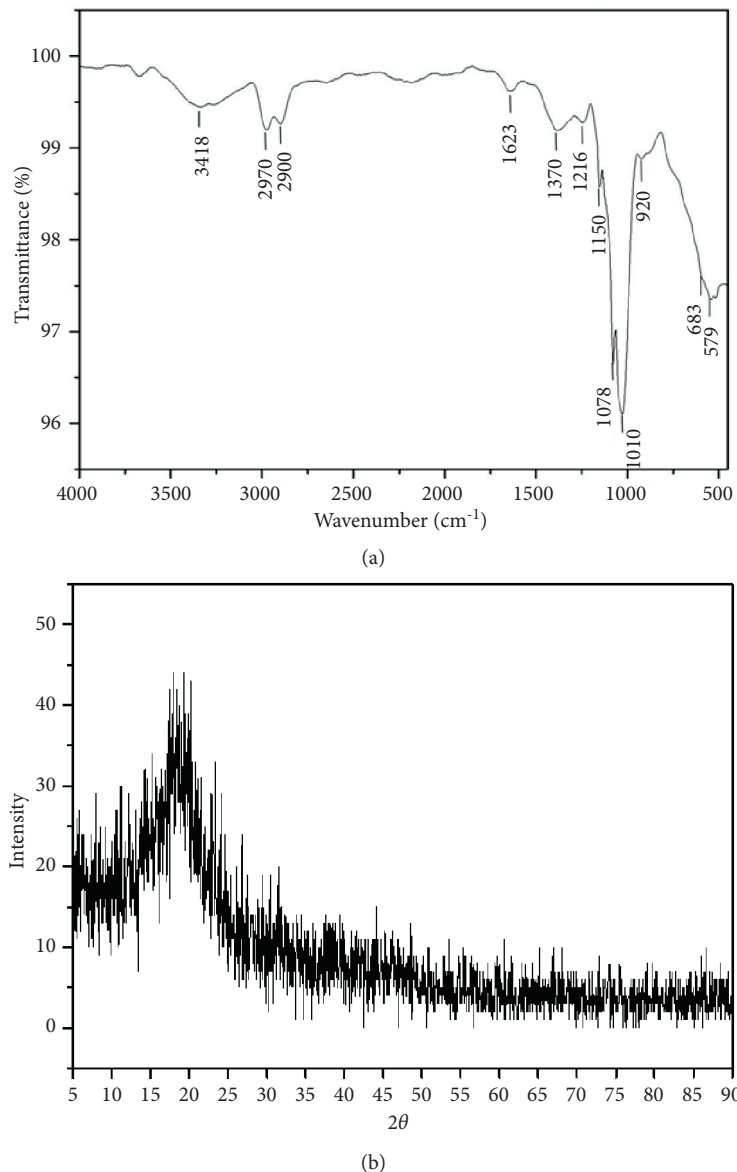


FIGURE 5: The structural characterization of TSP: (a) FT-IR spectroscopy of TSP, indicating different functional groups, and (b) XRD analysis of TSP.

solution increased. Gel structure was initially formed when the concentration was 15 mg/mL. Shear-thinning hydrocolloids were widely used to modify food texture. Hence, TSP (0.1–20 mg/mL) is promising to be used in the food field to improve the quality of food.

3.9. In Vitro Antioxidant Activity. In this experiment, to confirm the anti-oxidant activities of TSP *in vitro*, the DPPH radical scavenging activity and hydroxyl radical scavenging activity were determined, while the results were presented in Figure 7. The DPPH evaluation of free radical scavenging activity of TSP shows a dose-dependent manner in scavenging ability (Figure 7(a)). The scavenging rate of TSP

against DPPH radical directly increased with the increase in the TSP concentration, but the scavenging rate was lower than that of the ascorbic acid solution. Between 0 and 20.0 mg/mL of concentrations, the DPPH scavenging rates of ascorbic acid and TSP increased significantly, which were 0% to 77.93% and 0% to 54.93%, respectively. The concentration of the TSP at which the scavenging rate reached 50% was defined as the half-maximal effective concentration (EC_{50}). The EC_{50} of DPPH scavenging activity for TSP and ascorbic acid was 15.32 and 1.17 mg/mL, respectively, indicating that an effect of ascorbic acid on DPPH radical scavenging was more significant than that of TSP. DPPH is synthetic stable radicals with an unpaired electron, which can be used as a probe to evaluate free radical scavenging

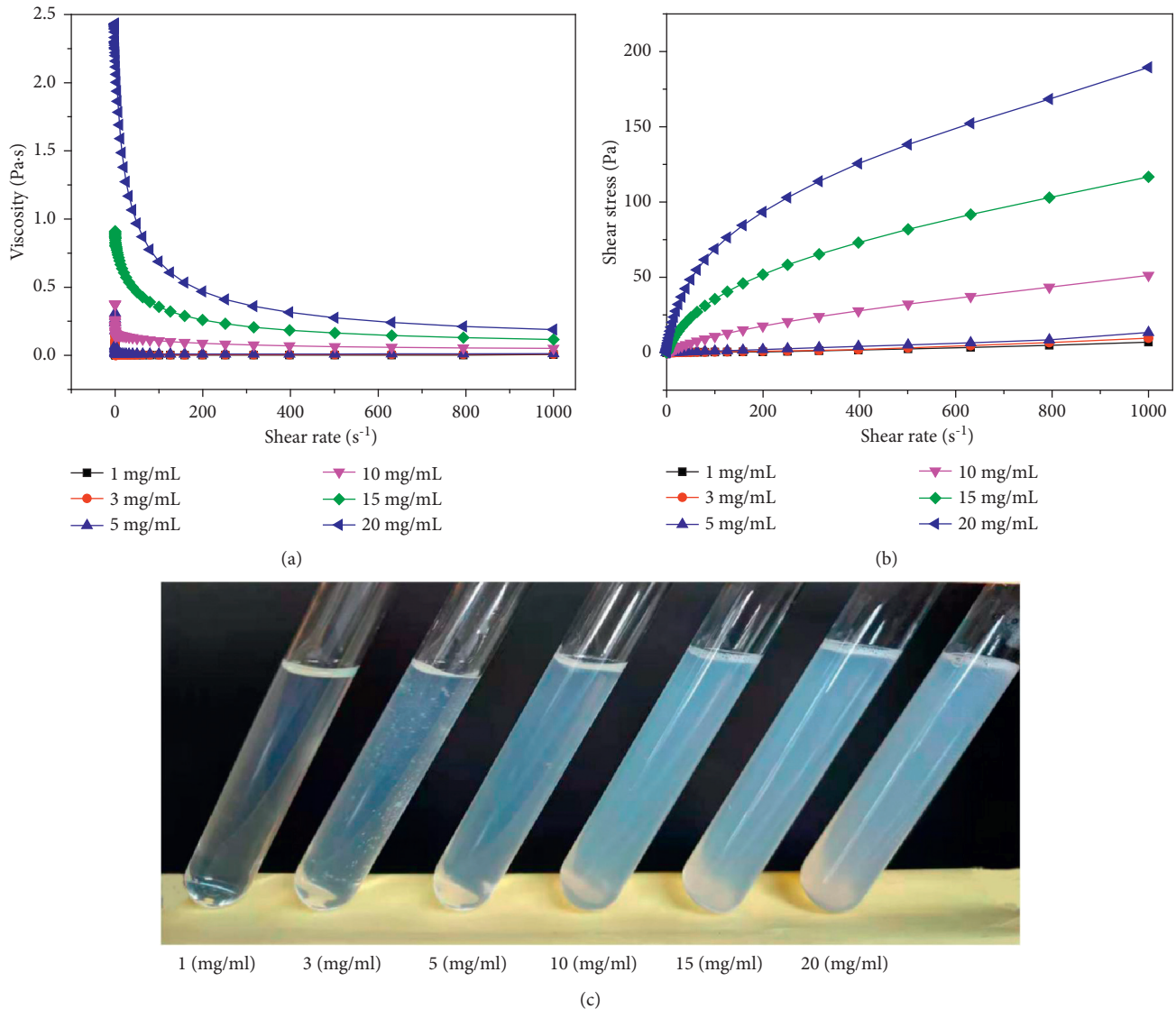


FIGURE 6: Shear rheology of different concentrations of TSP at 25°C: (a) curves of viscosity versus shear rate for TSP solutions with different concentrations (1–20 mg/mL), (b) curves of shear stress versus shear rate for TSP solutions with different concentrations (1–20 mg/mL), and (c) photos of TSP solutions at different concentrations.

TABLE 3: Power-law equations and parameters of the TSP.

TSP concentration (mg/mL)	K	n	R^2
1	0.0241 ^d	0.4539 ^d	0.6081
3	0.0146 ^d	0.6605 ^c	0.7152
5	0.0330 ^d	0.6774 ^c	0.8576
10	0.1784 ^c	0.8537 ^b	0.9790
15	0.4831 ^b	0.8464 ^b	0.9522
20	1.5773 ^a	0.9201 ^a	0.9779

a–d: statistical significance level of $p < 0.05$ calculated by Duncan's test.

activity. The anti-oxidant mechanisms of DPPH is a combination of both single electron transfer mechanism (SET) and hydrogen atom transfer (HAT) [45]. Hence, this ability may be related to the hydroxyl group of the TSP that can provide hydrogen to scavenge the DPPH radical [46].

Hydroxyl radicals can attack biological macromolecules and increase the risk of oxidative stress and lead to the occurrence of related diseases. The scavenging rate on hydroxyl radical is shown in Figure 7(b). The hydroxyl radical scavenging ability of TSP was less than that of ascorbic acid, and the scavenging rate of TSP and ascorbic acid were 0~27.43% and 0~72.34%, respectively. Moreover, both TSP and ascorbic acid were found to have an increased scavenging rate with the increase of the concentration and also exhibit a concentration-dependent manner. Compared with DPPH radical scavenging activity, TSP possessed lower scavenging activity against hydroxyl radicals.

An increasing number of studies confirm the role of polysaccharides in anti-oxidants, which was attributed to their molecular weight, uronic acid content, type of monosaccharide, and glycosidic linkage [47]. In the FT-IR

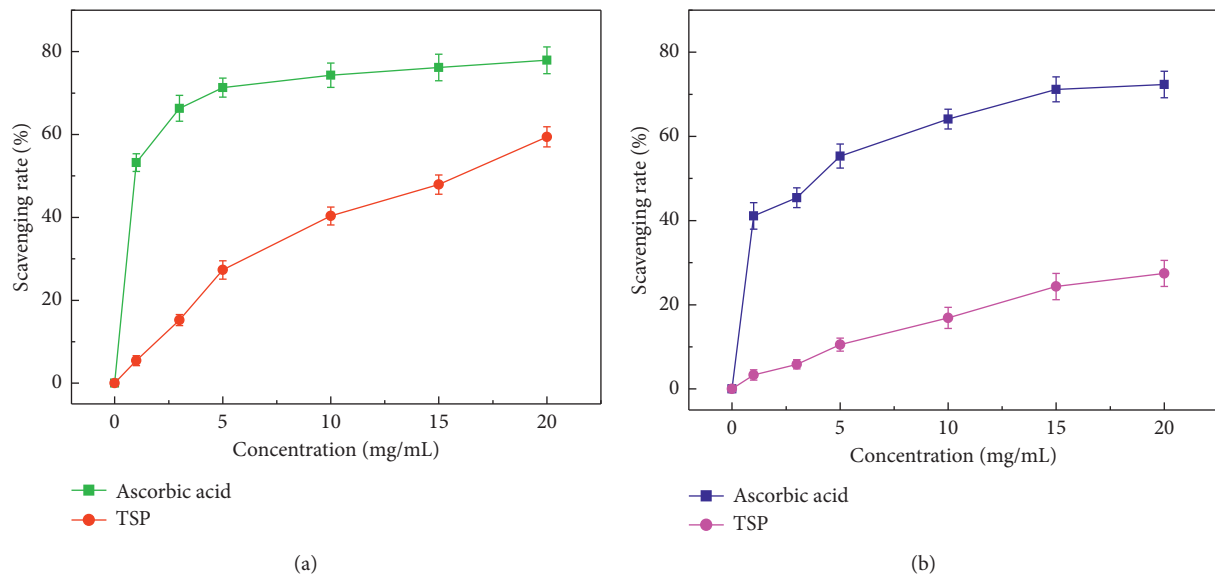


FIGURE 7: Antioxidant activity of TSP *in vitro*: (a) scavenging rate on DPPH radical and (b) scavenging rate on hydroxyl radical. Statistical significance level of $p < 0.05$ calculated by Duncan's test.

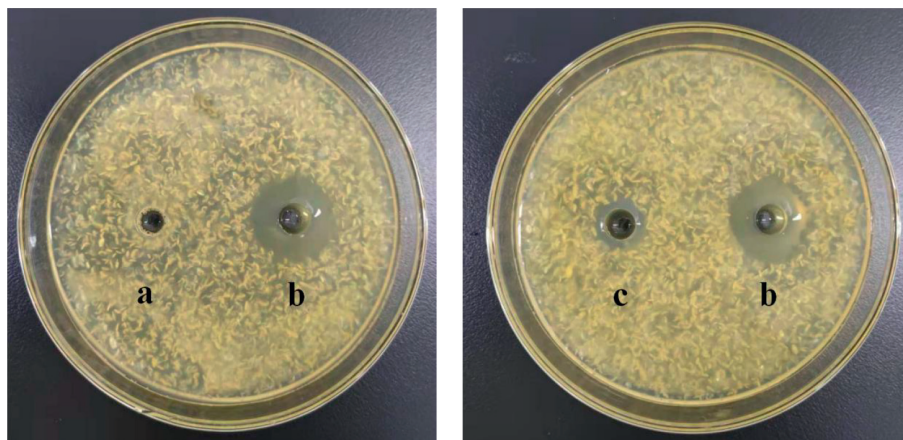


FIGURE 8: Antibacterial activity of TSP toward *Escherichia coli* bacterial strains: (a) dH₂O treat, (b) chitosan treat, and (c) TSP treat.

analysis, we found TSP was composed of configuration in pyranose form sugars that have been verified to possess stronger antioxidant activity revealed by Luo et al. [48]. Monosaccharide compositions of the polysaccharides have a great impact on their antioxidant activities [49]. The antioxidant activity of polysaccharides and the content of uronic acid in pumpkin seeds were determined by Buathongjan et al. [50], and the results showed that the anti-oxidant activity was directly proportional to the glucuronic acid content. In this work, the results of monosaccharide composition showed the contents of uronic acid (0.5%) in TSP. Moreover, the OH group was also present, which can react with radical. All of these may be the reason for the antioxidant activity of TSP. However, the specific mechanism of antioxidant activity of TSP remains to be further investigated.

3.10. Antibacterial Activity. The anti-microbial activity of TSP against *E. coli* was tested. Our pre-experiment showed that a low concentration of TSP had no anti-bacterial effect, so 20 mg/ml TSP solution was used to explore in the present study. The anti-bacterial effects of TSP on *E. coli* were assessed according to the size of the inhibition zone. As shown in Figure 8, it was obvious that the TSP exhibited good anti-microbial activity against *E. coli*. Specifically, there was no inhibition zone in the water treatment group. On the contrary, chitosan showed a larger inhibition zone. The inhibition zones were significantly reduced in the experimental group (TSP), indicating that TSP had a certain inhibitory activity on the bacteria. This result was in agreement with the finding of Ding et al. and Wang et al. [4, 18] who revealed that polysaccharides isolated from plant seed had anti-bacterial activity against Gram-positive and Gram-

negative bacteria. Thus, it was testified that TSP showed potent activity to inhibit Gram-negative bacteria (*E. coli*). The antibacterial activity against Gram-positive TSP will continue to be explored in the future. Previous studies have shown that the antibacterial activity of polysaccharides could be related to membrane permeable properties. The polysaccharide can act on the cell wall and destroy membrane structure, causing a large amount of biological macromolecule leakage and affecting its metabolic activity [51]. Thus, we speculated that the anti-microbial activity of TSP might be attributed to the membrane permeability. Moreover, according to a previous report, the content of uronic acid and charge type in polysaccharides can influence antibacterial activity [52]. TSP contains uronic acid, and the results of ζ potential showed that TSP was a kind of polyanion polysaccharide, which could attack the positively charged membrane proteins and lead to bacteria apoptosis [53]. However, this hypothesis about anti-bacterial mechanisms remains to be further investigated. The present results also showed tamarind seeds were the potential source for the production of active polysaccharides and confirmed that TSP can also act as a promising anti-microbial agent.

4. Conclusions

The characterization of TSP showed a typical FTIR spectrum characteristic of polysaccharides and the XRD picture revealed the amorphous behavior. Moreover, TSP morphology displayed rough, tight, and uneven. However, further studies are required to investigate the holistic structure of TSP. Furthermore, the results of function and biological activity suggested that TSP possessed pseudo-plastic characteristics, while it showed good anti-oxidant and anti-bacterial activities against Gram-negative bacteria. These results can provide a reference for the efficient utilization of tamarind seed and may guide further works concerning tamarind seed polysaccharides, enabling its development and application in the food industry.

Data Availability

The data used to support the findings of this study are included within the article.

Conflicts of Interest

The authors declare that there are no conflicts of interest.

Authors' Contributions

Likun Ren and Yang Yang contributed equally to this work.

Acknowledgments

The authors appreciate the financial support from the National Natural Science Foundation of China (32072258), Major Science and Technology Program of Heilongjiang (2020ZX08B02), and Harbin University of Commerce "young innovative talents" support program (2019CX06 and

2020CX26), central financial support for the development of local colleges and universities.

References

- [1] H. E. Tahir, Z. Xiaobo, G. K. Mahunu, M. Arslan, M. Abdalhai, and L. Zhihua, "Recent developments in gum edible coating applications for fruits and vegetables preservation: a review," *Carbohydrate Polymers*, vol. 224, no. 15, Article ID 115141, 2019.
- [2] C. Soukoulis, C. Gaiani, and L. Hoffmann, "Plant seed mucilage as emerging biopolymer in food industry applications," *Current Opinion in Food Science*, vol. 22, pp. 28–42, 2018.
- [3] Q. Jin, Z. Cai, X. Li, M. P. Yadav, and H. Zhang, "Comparative viscoelasticity studies: corn fiber gum versus commercial polysaccharide emulsifiers in bulk and at air/liquid interfaces," *Food Hydrocolloids*, vol. 64, pp. 85–98, 2017.
- [4] J. Ding, H. Zhang, Y. Tian, P. F. H. Lai, H. Xu, and L. Ai, "Rheological properties of *Prunus persica* exudate: potential effects of proteins and polyphenols," *International Journal of Biological Macromolecules*, vol. 133, no. 15, pp. 831–838, 2019.
- [5] S. Muthusamy, G. P. Udayakumar, and V. R. Narala, "Recent advances in the extraction and characterization of seed polysaccharides, and their bioactivities: a review," *Bioactive Carbohydrates and Dietary Fibre*, vol. 26, Article ID 100276, 2021.
- [6] Y. Sudjaroen, R. Haubner, G. Würtele et al., "Isolation and structure elucidation of phenolic antioxidants from Tamarind (*Tamarindus indica* L.) seeds and pericarp," *Food and Chemical Toxicology*, vol. 43, no. 11, pp. 1673–1682, 2005.
- [7] T. Phakruschaphan, "Comparison of peeling and extraction methods in the production of Tamarind seed gum," *The Kasetsart Journal of Natural Sciences*, vol. 16, no. 2, pp. 74–81, 1982.
- [8] P. Bharat Helkar, A. Sahoo, and N. J. Patil, "Review: food industry by-products used as a functional food ingredients," *International Journal of Wine Research*, vol. 6, no. 3, Article ID 1000248, 2016.
- [9] B. B. Mangsingh, J. S. Binoj, N. P. Sai et al., "Sustainable development in utilization of *Tamarindus indica* L. and its by-products in industries: a review," *Current Research in Green and Sustainable Chemistry*, vol. 4, Article ID 100207, 2021.
- [10] C. Khanittha, S. Patsuda, and K. Praphakorn, "Extraction and characterization of tamarind (*Tamarindus indica* L.) seed polysaccharides (TSP) from three difference sources," *Molecules*, vol. 21, no. 6, 2016.
- [11] H. Shao, H. Zhang, Y. Tian, Z. Song, P. Lai, and L. Ai, "Composition and rheological properties of polysaccharide extracted from tamarind (*Tamarindus indica* L.) seed," *Molecules*, vol. 24, no. 7, p. 1218, 2019.
- [12] S. Jana, A. Banerjee, K. K. Sen, and S. Maiti, "Gelatin-carboxymethyl tamarind gum biocomposites: in vitro characterization & anti-inflammatory pharmacodynamics," *Materials Science and Engineering: C*, vol. 69, no. 1, pp. 478–485, 2016.
- [13] S. Periasamy, C.-H. Lin, B. Nagarajan, N. V. Sankaranarayanan, U. R. Desai, and M.-Y. Liu, "Tamarind xyloglucan attenuates dextran sodium sulfate induced ulcerative colitis: role of antioxidation," *Journal of Functional Foods*, vol. 42, pp. 327–338, 2018.
- [14] M. Heydarian, H. Jooyandeh, B. Nasehi, and M. Noshad, "Characterization of *Hypericum perforatum* polysaccharides with antioxidant and antimicrobial activities: optimization based statistical modeling," *International Journal of Biological Macromolecules*, vol. 104, pp. 287–293, 2017.

- [15] Y. Zhang, D. Y. Mi, J. Wang et al., "Constituent and effects of polysaccharides isolated from sophora moorcroftiana seeds on lifespan, reproduction, stress resistance, and antimicrobial capacity in caenorhabditis elegans," *Chinese Journal of Natural Medicines*, vol. 16, no. 6, pp. 252–260, 2018.
- [16] X.-L. Li, K. Thakur, Y.-Y. Zhang et al., "Effects of different chemical modifications on the antibacterial activities of polysaccharides sequentially extracted from peony seed dreg," *International Journal of Biological Macromolecules*, vol. 116, pp. 664–675, 2018.
- [17] Y. Chai and M. Zhao, "Purification, characterization and anti-proliferation activities of polysaccharides extracted from *Viscum coloratum* (Kom.) Nakai," *Carbohydrate Polymers*, vol. 149, pp. 121–130, 2016.
- [18] L. Wang, F. Liu, A. Wang, Z. Yu, Y. Xu, and Y. Yang, "Purification, characterization and bioactivity determination of a novel polysaccharide from pumpkin (*Cucurbita moschata*) seeds," *Food Hydrocolloids*, vol. 66, pp. 357–364, 2017.
- [19] K. Jahanbin, S. Moini, A. R. Gohari, Z. Emam-djomeh, and P. Masi, "Isolation, purification and characterization of a new gum from *Acanthophyllum bracteatum* roots," *Food Hydrocolloids*, vol. 27, no. 1, pp. 14–21, 2012.
- [20] M. Dubois, K. A. Gilles, J. K. Hamilton, P. A. Rebers, and F. Smith, "Colorimetric method for determination of sugars and related substances," *Analytical Chemistry*, vol. 28, no. 3, pp. 350–356, 1956.
- [21] N. Blumenkrantz and G. Asboe-Hansen, "New method for quantitative determination of uronic acids," *Analytical Biochemistry*, vol. 54, no. 2, pp. 484–489, 1973.
- [22] C. Wang, Y. He, X. Tang, and N. Li, "Sulfate, structural analysis, and anticoagulant bioactivity of ginger polysaccharides," *Journal of Food Science*, vol. 85, no. 6, pp. 2427–2434, 2020.
- [23] T. Kaewmanee, L. Bagnasco, S. Benjakul et al., "Characterisation of mucilages extracted from seven Italian cultivars of flax," *Food Chemistry*, vol. 148, pp. 60–69, 2014.
- [24] L. Zhang, Y. Hu, X. Duan et al., "Characterization and antioxidant activities of polysaccharides from thirteen boletus mushrooms," *International Journal of Biological Macromolecules*, vol. 113, pp. 1–7, 2018.
- [25] X. Li, R. Guo, X. Wu et al., "Dynamic digestion of tamarind seed polysaccharide: indigestibility in gastrointestinal simulations and gut microbiota changes *in vitro*," *Carbohydrate Polymers*, vol. 239, Article ID 116194, 2020.
- [26] M. J. Gidley, P. J. Lillford, D. W. Rowlands et al., "Structure and solution properties of tamarind-seed polysaccharide," *Carbohydrate Research*, vol. 214, no. 2, pp. 299–314, 1991.
- [27] S. K. Abdullaev, "D-xylose study of the absorptive function of the small intestine in children with dysentery," *Pediatrics*, vol. 57, no. 6, pp. 39–52, 1978.
- [28] G. Crispín-Isidro, L. Hernández-Rodríguez, C. Ramírez-Santiago, O. Sandoval-Castilla, C. Lobato-Calleros, and E. J. Vernon-Carter, "Influence of purification on physicochemical and emulsifying properties of tamarind (*Tamarindus indica* L.) seed gum," *Food Hydrocolloids*, vol. 93, pp. 402–412, 2019.
- [29] C.-F. Mao, M.-C. Hsu, and W.-H. Hwang, "Physicochemical characterization of grifolan: thixotropic properties and complex formation with Congo Red," *Carbohydrate Polymers*, vol. 68, no. 3, pp. 502–510, 2007.
- [30] J. I. Acedo-Carrillo, A. Rosas-Durazo, R. Herrera-Urbina, M. Rinaudo, F. M. Goycoolea, and M. A. Valdez, "Zeta potential and drop growth of oil in water emulsions stabilized with mesquite gum," *Carbohydrate Polymers*, vol. 65, no. 3, pp. 327–336, 2006.
- [31] M. Danaei, M. Dehghankhold, S. Ataei et al., "Impact of particle size and polydispersity index on the clinical applications of lipidic nanocarrier systems," *Pharmaceutics*, vol. 10, no. 2, pp. 57–73, 2018.
- [32] Y. Pan, C. Wang, Z. Chen, W. Li, G. Yan, and H. Chen, "Physicochemical properties and antidiabetic effects of a polysaccharide from corn silk in high-fat diet and streptozotocin-induced diabetic mice," *Carbohydrate Polymers*, vol. 164, no. 15, pp. 370–378, 2017.
- [33] F. Rashid, S. Hussain, and Z. Ahmed, "Extraction purification and characterization of galactomannan from fenugreek for industrial utilization," *Carbohydrate Polymers*, vol. 180, pp. 88–95, 2018.
- [34] M. Meng, D. Cheng, L. Han, Y. Chen, and C. Wang, "Isolation, purification, structural analysis and immunostimulatory activity of water-soluble polysaccharides from *Grifola frondosa* fruiting body," *Carbohydrate Polymers*, vol. 157, pp. 1134–1143, 2017.
- [35] N. Farhadi, "Structural elucidation of a water-soluble polysaccharide isolated from Balangu shirazi (*Lallemantia royleana*) seeds," *Food Hydrocolloids*, vol. 72, pp. 263–270, 2017.
- [36] Z. H. Tang, H. W. Gao, S. Wang, S. H. Wen, and S. Qin, "Hypolipidemic and antioxidant properties of a polysaccharide fraction from *Enteromorpha prolifera*," *International Journal of Biological Macromolecules*, vol. 58, pp. 186–189, 2013.
- [37] S. R. Thambaraj, N. Reddy, M. Phillips, and S. R. Koyyalamudi, "Biological activities and characterization of polysaccharides from the three Australian Sweet Lupins," *International Journal of Food Properties*, vol. 22, no. 1, pp. 522–535, 2019.
- [38] L. Yang and L. M. Zhang, "Chemical structural and chain conformational characterization of some bioactive polysaccharides isolated from natural sources," *Carbohydrate Polymers*, vol. 76, pp. 349–361, 2008.
- [39] A. Savi, G. C. Calegari, V. A. Q. Santos, E. A. Pereira, and S. D. Teixeira, "Chemical characterization and antioxidant of polysaccharide extracted from *Dioscorea bulbifera*," *Journal of King Saud University Science*, vol. 32, no. 1, pp. 636–642, 2020.
- [40] S. Basu, M. Ghosh, R. K. Bhunia, J. Ganguly, and B. K. Banik, "Polysaccharides from *Dolichos biflorus* Linn and *Trachyspermum ammi* Linn seeds: isolation, characterization and remarkable antimicrobial activity," *Chemistry Central Journal*, vol. 11, no. 1, pp. 118–128, 2017.
- [41] B. S. Chagas, D. L. P. Machado, R. B. Haag, C. R. D. Souza, and E. F. Lucas, "Evaluation of hydrophobically associated polyacrylamide-containing aqueous fluids and their potential use in petroleum recovery," *Journal of Applied Polymer Science*, vol. 91, no. 6, pp. 3686–3692, 2004.
- [42] M. Tabarsa, M. Anvari, H. S. Joyner, S. Behnam, and A. Tabarsa, "Rheological behavior and antioxidant activity of a highly acidic gum from *Althaea officinalis* flower," *Food Hydrocolloids*, vol. 69, pp. 432–439, 2017.
- [43] S. He, X. Wang, Y. Zhang et al., "Isolation and prebiotic activity of water-soluble polysaccharides fractions from the bamboo shoots (*Phyllostachys praecox*)," *Carbohydrate Polymers*, vol. 151, pp. 295–304, 2016.
- [44] E. Alpizar-Reyes, A. Román-Guerrero, R. Gallardo-Rivera, V. Varela-Guerrero, J. Cruz-Olivares, and C. Pérez-Alonso, "Rheological properties of tamarind (*Tamarindus indica* L.) seed mucilage obtained by spray-drying as a novel source of hydrocolloid," *International Journal of Biological Macromolecules*, vol. 107, pp. 817–824, 2017.

- [45] S. Pandey, N. Chaturvedi, and D. Gupta, "Impact of malting on antioxidant content and DPPH scavenging activity of medicago sativa," *International Journal of Current Microbiology and Applied Sciences*, vol. 9, no. 2, pp. 262–267, 2020.
- [46] B. Yang, M. Zhao, N. Prasad, G. Jiang, and Y. Jiang, "Effect of methylation on the structure and radical scavenging activity of polysaccharides from longan (*Dimocarpus longan* Lour.) fruit pericarp," *Food Chemistry*, vol. 118, no. 2, pp. 364–368, 2010.
- [47] J. Shi, J. Zhang, Y. Sun et al., "Physicochemical properties and antioxidant activities of polysaccharides sequentially extracted from peony seed dreg," *International Journal of Biological Macromolecules*, vol. 91, pp. 23–30, 2016.
- [48] A. Luo, X. He, S. Zhou, Y. Fan, A. Lou, and Z. Chu, "Purification, composition analysis and antioxidant activity of the polysaccharides from *Dendrobium nobile* Lindl.," *Carbohydrate Polymers*, vol. 79, no. 4, pp. 1014–1019, 2010.
- [49] X. Li, S. Chen, J. Li et al., "Chemical composition and antioxidant activities of polysaccharides from Yingshan cloud mist tea," *Oxidative Medicine and Cellular Longevity*, vol. 2019, Article ID 1915967, 11 pages, 2019.
- [50] C. Buathongjan, K. Israkarn, W. Sangwan, T. Qutrequin, C. Gamonpilas, and P. Methacanon, "Studies on chemical composition, rheological and antioxidant properties of pectin isolated from Riang (*Parkia timoriana* (DC.) Merr.) pod," *International Journal of Biological Macromolecules*, vol. 164, pp. 575–4582, 2020.
- [51] L. Xue, J. Long, C. Lu, X. F. Li, X. M. Xu, and Z. Y. Jin, "Immobilization of polygalacturonase for the preparation of pectic oligosaccharides from mango peel wastes and assessment of their antibacterial activities," *Food Bioscience*, vol. 39, Article ID 100837, 2021.
- [52] X. Chen, L. Tao, Y. Ru et al., "Antibacterial mechanism of *Tetrastigma hemsleyanum* Diels et Gilg's polysaccharides by metabolomics based on HPLC/MS," *International Journal of Biological Macromolecules*, vol. 140, pp. 206–215, 2019.
- [53] M. Liu, Y. Liu, M. J. Cao et al., "Antibacterial activity and mechanisms of depolymerized fucoidans isolated from *Laminaria japonica*," *Carbohydrate Polymers*, vol. 172, pp. 294–305, 2017.